Hindawi
Journal of Chemistry
Volume 2019, Article ID 6480354, 9 pages
https://doi.org/10.1155/2019/6480354

Research Article

Kraft Lignin Conversion into Energy Carriers under the Action of Electromagnetic Radiation

P. Zharova, O. V. Arapova, G. I. Konstantinov, A. V. Chistyakov, and M. V. Tsodikov

A. V. Topchiev Institute of Petrochemical Synthesis Russian Academy of Sciences, Moscow, Russia

Correspondence should be addressed to A. V. Chistyakov; chistyakov@ips.ac.ru

Received 29 November 2018; Accepted 8 January 2019; Published 20 February 2019

Academic Editor: Daniele Dondi

Copyright © 2019 P. Zharova et al. This is an open access article distributed under the Creative Commons Attribution License, which permits unrestricted use, distribution, and reproduction in any medium, provided the original work is properly cited.

In this work, it was found that the deposition of iron salts (iron acetate) on kraft lignin at extremely low concentrations of 0.1 wt.% leads to a sharp increase in the absorbing capacity of microwave radiation by kraft lignin at its power of 1 kW and the conversion of kraft lignin to a hydrogen-containing gas with the degree of hydrogen extraction, reaching 90% based on the hydrogen contained in the kraft lignin. It has been established that the deposition of metals (Fe and Ni) on kraft lignin allows one to directionally change the selectivity of the process of its destruction under the influence of microwave radiation, which makes it possible to classify the process as plasmacatalytic. The results obtained make it possible to minimize the amount of catalyst used and propose an efficient way of producing hydrogen from kraft lignin waste.

1. Introduction

One of the priorities in the field of petrochemistry and energy is the development of efficient approaches for the production of hydrogen and synthesis gas as the most environmentally friendly energy carriers. The processing of hydrocarbons into hydrogen and synthesis gas is among the strategically important industrial production of major energy sources in all developed countries of the world.

Kraft lignin is a natural polymer consisting of phenylpropane structures. It is the building material of plant cells and fibers. In the wood of various species, the kraft lignin content varies from 20 to 40% [1]. About 70 million tons of kraft lignin waste, mainly kraft lignin, which is a by-product of pulp production, is generated abroad every year [2, 3]. It should be particularly noted that sulfur-containing kraft lignin (to which kraft lignin belongs) is not recycled, as a result of which significant amounts accumulate. Only in the territory of the Russian Federation, more than 95 million tons of kraft lignin has been accumulated as waste at a pulp and paper mill [3].

From the point of view of the chemical industry, kraft lignin is a promising raw material for the production of a wide range of aromatics that can be used as components of fuels or valuable chemical compounds. Currently, the development of efficient technology for the processing of kraft lignin is one of the most important problems facing humanity from the point of view of sustainable development and the global economy. The scientific community is working on several main channels of kraft lignin utilization, such as pyrolysis and gasification, aimed at producing hydrogen-containing gas and bio-oils, hydrogenolysis for the production of individual aromatics, and oxidation, whose products are carbon oxides and aromatic and aliphatic alcohols [4].

In the framework of the development of pyrolysis and gasification of kraft lignin, a special place is occupied by the use of microwave radiation, which is a source of energy and at the same time initiates polarization and repolarization of the functional groups of substrate molecules, which leads to an intensification of the breakdown of kraft lignin polymeric structures [5].

Directly, kraft lignin has a low tangent of dielectric loss angle of 0.15–0.25 and, as a result, has an extremely low ability to absorb microwave radiation [6]. As a result, to initiate the cracking process of kraft lignin, it is necessary to supply a high-power radiation of ~6 kW [7] or use catalysts that are capable of absorbing microwaves [8–10]. Carbon-

based materials [8] or mixed metal oxides [9, 10] are used as such materials. The disadvantage of the systems used is the complexity of their preparation and the high content in the reaction mass (20 wt.% or more), as well as the impossibility of their regeneration to the active state [11].

This paper proposes a method for modifying kraft lignin with iron salts in order to increase its ability to absorb microwave radiation and a comparative analysis of the kraft lignin conversion process under the action of microwave radiation with applied metal particles, with the addition of a carbon absorber of electromagnetic waves and in convective heating.

2. Experimental

2.1. Materials. Kraft lignin obtained at the Kirov wood processing plant (Russia) was used as a reagent. The composition of the initial kraft lignin, determined by C, H, N, and S analysis on the instrument C, H, N, S-OEA1108-Elemental Analyzer with chromatographic termination (PROPA-Q-10, He, katharometer), was as follows in wt.%: C-58.1, H-5.4, Al-1.2, Si-3.1, Ca-0.6, Fe-0.8, Mg-0.04, S-1.2, N-0.2, O-28.9, and the rest-0.5 (the content of each component is less than 0.05%).

As a sorbent of microwave radiation, spherical gas coal (SGC) was added to the reactor, with a granule diameter of 2-3 mm. Characteristics of the SGC carbon material are as follows: ash content (A^d): 14%, total pore volume (V_Σ): 1.52 cm^3/g, sorbing pore volume (V_S): 0.52 cm^3/g, and macropore volume (V_{ma}): 1.00 cm^3/g.

The application of metals on the kraft lignin was carried out by the method of impregnation on the capacity. Ferric acetate Fe $(OAc)_3$ (Aldrich, 97%) and Ni acetate $(OAc)_2 \times 4H_2O$ (Aldrich, 98%) were used as starting salts for deposition. Salts were applied from aqueous solutions; the water capacity of kraft lignin in water was 4 cm^3/g. The moist kraft lignin was dried in air at room temperature for 24 hours and in a drying oven at 110°C for two hours.

Also, by the impregnation method, combined samples were prepared containing 1.5% Ni + 0.5% Fe and 0.1% Fe + 1.5% Ni, in which the deposition of metals took place in two stages. In the first stage, 1.5% Ni and 0.1% Fe were deposited, followed by drying. In the second stage, 0.5% Fe and 1.5% Ni were deposited on the metal-containing kraft lignin, after which the samples were dried.

The actual metal content in the prepared samples was determined using atomic absorption spectrometry (AAS) on a Thermo iCE 3000 instrument. The relative error in the measurement of metal content using the AAS method is equal to ±1%.

2.2. Experiments. Experiments on the conversion of kraft lignin were carried out at the microwave generation installation shown in Figure 1. As a microwave source, a 1-kW M-140 magnetron used in household microwave ovens generating microwave radiation with a frequency of 2.45 ± 0.05 GHz and a current density of 100–150 mA was used. The power supply circuit of the anode of the magnetron is provided from the output of a half-wave rectifier with voltage doubling, and the unit is powered from an AC network with a voltage of 220 V (50 Hz). The voltage is regulated by using a transformator, which allows you to control the level of generated power over a wide range. The power of the supplied radiation was varied using the current density control. The power supply of the magnetron provides automatic switching off of the anode voltage in the event of deviation of the specified forced process modes and spontaneous violation of the set power mode of the magnetron along the anode circuit. To measure the temperature of the reaction zone, tungsten-rhenium thermocouple was used, which was installed in the reactor pocket at 1/2 the height of the reaction zone. The microwave-induced temperature at a given current density was maintained using an automatic magnetron switch-on regulator.

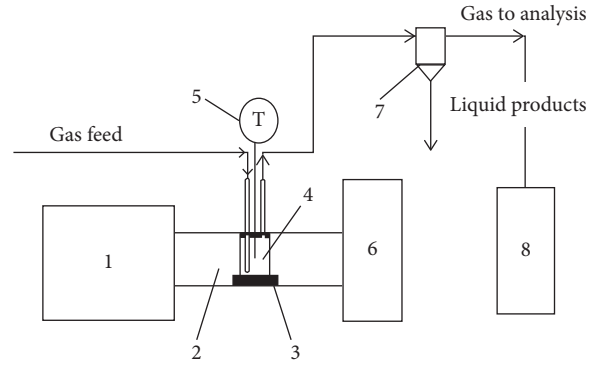

Figure 1: Schematic diagram of the installation for the processing of kraft lignin under the action of microwave radiation. 1: magnetron and power supply; 2: waveguide; 3: absorbing ceramics; 4: quartz reactor; 5: thermocouple; 6: residual MWI absorption chamber; 7: cooled separator; 8: gas chromatograph.

To carry out the conversion of kraft lignin, a quartz reactor (4) of a flow type with a volume of 15 cm^3 was installed on a ceramic substrate (3) in the direction of the electromagnetic waves generated by the magnetron (1). At the exit of the reactor, the residual radiation was absorbed by water (6). In a typical experiment, CO_2 was supplied through the reactor with kraft lignin samples to the lower part of the reactor at a rate of 60°cm^3/min at an induced temperature of 700–750°C. Upon reaching the operating mode, the selection of decomposition products began, which lasted until the end of the experiment. The exposure time in the operating mode in all experiments was 10 min.

To compare the effectiveness of microwave exposure with traditional thermal heating, the installation equipped with a convective heating furnace was used; the installation diagram is shown in Figure 2.

Experiments on the conversion of kraft lignin during convective heating were carried out in a quartz reactor, which was placed in a furnace heated to 750 or 800°C, and the supply of CO_2 was 60 cm^3/min and kept for 15 minutes. Gaseous reaction products were analyzed by the method of gas chromatography in the "online" mode.

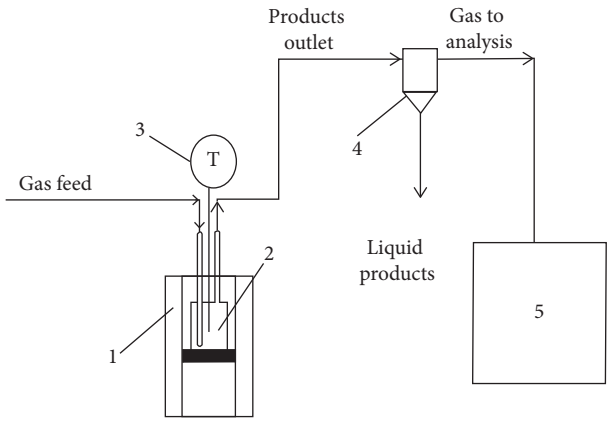

Figure 2: Diagram of the experimental installation of convective heating. 1: radial oven convective heating; 2: quartz reactor; 3: temperature regulator; 4: cooled separator; 5: chromatograph.

2.3. Catalysts Characterization. The ^{57}Fe Mössbauer spectra were obtained on a Wissel electrodynamic-type spectrometer (Germany) at a temperature of 300 K. ^{57}Co (Rh) with an activity of 1.1 GBq was used as a radiation source. The isomeric shifts were counted from the center of the magnetic hyperfine structure of metallic iron. Mössbauer spectra were processed according to standard OLS programs (LOREN-IChPh RAS, NORMOS-Germany) under the assumption of the Lorentz line shape.

High-resolution transmission electron microscopy was carried out on a JEM-2010 microscope ("JEOL") with a resolution of 0.14 nm on a grating and an accelerating voltage of 200 kV. X-ray energy dispersive analysis (EDA) was performed using an EDAX microscope attachment (EDAX Co) and an X-ray microanalyzer with a semiconductor Si (Li) detector with a resolution of ~130 eV. The size of the deposited particles of the active component was determined as the maximum linear size. To construct histograms of particle size distributions, data related to 192–243 particles were processed by a statistical method.

2.4. Products Analysis. Analysis of C_1–C_5 hydrocarbon gases was performed on a Crystal-4000 chromatograph (FID, He 70 cm^3/min; 120°C; P 1.65 MPa, HP-PLOT/Al_2O_3, 50 m × 0.32 mm).

The analysis of CO, CO_2, and H_2 was carried out on a Kristall-4000 chromatograph (Katarometr, Ar, SKT column, 150 × 0.4 cm, 130°C, 30 ml/min).

The quantitative composition of liquid organic reaction products was determined by GLC on a Varian 3600, column: Hromtek SE-30, 0.25 mm × 25 m, $D_f = 0.3\ \mu$m, 50°C (5 min), 10°/min, 280°C, $t_{inzh} = 250$°C, $R_{inzh} = 1$ bar, dividing the flow 1/200, PID.

The study of the composition of the mixture of liquid reaction products was carried out on a Thermo Focus DSQ II chromatomass spectrometer (Varian VF-5 ms capillary column, 30 m long, 0.25 mm internal diameter, 0.25 phase thickness, 70 eV ionization energy, 230°C source temperature, 10–400 Da at a speed of 2 scans/s, resolution is one over the entire mass range). For the identification of components, used reference mass spectra presented in the NIST/EPA/NIH 17 database.

2.5. Equations for Process Parameters. To estimate the conversion parameters for microwave radiation, the following formulas were used:

Conversion of the organic part of kraft lignin (%):

$$x = \frac{m_{\text{init}} - m_{\text{res}}}{m_{\text{init}} - m_{\text{inorg}} - m_{\text{Ni}}} \cdot 100\%, \quad (1)$$

where m_{init} is the mass of the original kraft lignin; m_{res} is a solid residue obtained after reforming; m_{inorg} is the mass of inorganic impurities; m_{Ni} is the mass of supported nickel. Conversion of kraft lignin to hydrogen (%):

$$x_{H_2} = \frac{m_{H_2\text{init}} - m_{H_2\text{res}}}{m_{H_2\text{init}}} \cdot 100\%, \quad (2)$$

where $m_{H_2\text{init}}$ and $m_{H_2\text{res}}$ are the mass of hydrogen in the original kraft lignin and the solid residue, respectively;

Selectivity for synthesis gas (%):

$$S_{H_2+CO} = \frac{\nu_{H_2} + \nu_{CO}}{\nu_{H_2} + \nu_{CO} + \nu_{CH_4} + \nu_{C_2-C_4}} \cdot 100\%, \quad (3)$$

where ν_{H_2}, ν_{CO}, ν_{CH_4}, and $\nu_{C_2-C_4}$ are the mole fractions of hydrogen, carbon monoxide, methane, and C_2–C_4 hydrocarbons, respectively.

3. Results and Discussion

The dynamics of heating of various samples subjected to microwave radiation are presented in Figure 3. As can be seen from Figure 3, the initial kraft lignin does not have a sufficient level of absorption of microwave radiation, and therefore, its conversion was carried out in a mixture with a carbon adsorbent.

In a carbon dioxide atmosphere, unmodified kraft lignin in the presence of carbon material (SGC) is converted into microwave liquid fraction and water, gaseous products, and solid residue. As shown by chromatography-mass spectrometry and IR-spectroscopy, the fraction of liquid hydrocarbons consists mainly of phenyl, guaiacil, and vanillin derivatives, which is observed in most works on the destruction of kraft lignin [12]. Gaseous products are mainly represented by hydrogen and carbon monoxide, the selectivity of formation of which is 36.8%, as well as by light hydrocarbons C_1–C_4 (Table 1).

The solid residue according to IR and Raman spectroscopy data is imperfect graphite-like and polyphenylene oxide structures. The degree of hydrogen extraction is 75.5%, while the molar ratio $H_2/CO = 0.6$. Replacing the carbon dioxide gas atmosphere with argon leads to an increase in the yield of liquid products from 22.1 to 41.7% and a decrease in the yield of gaseous products by 10%. When exposed to microwave radiation on a mechanical mixture of kraft lignin with a carbon sorbent, the plasma is ignited in the pores of the sorbent, from where thermal energy is transferred to the entire volume of the reactor. The phenomenon of plasma ignition in sorbent pores was investigated earlier [13]. In fact, with such an organization

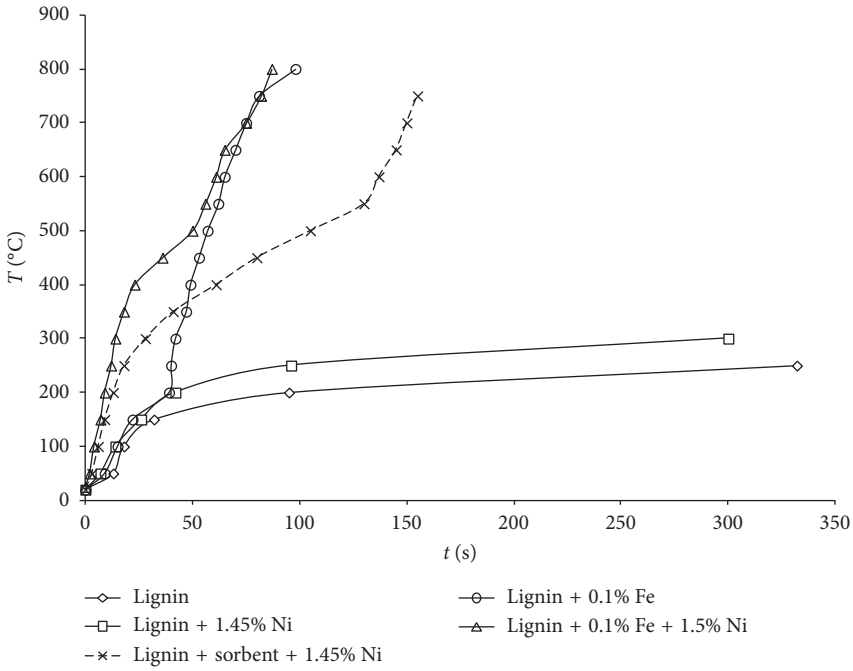

Figure 3: Dynamics of heating of kraft lignin samples.

Table 1: Material balance of kraft lignin conversion.

Number	Content of active ingredients (wt.%)	Gas atmosphere	Liquid product (wt.%)	Gaseous products (wt.%)	Solid residue (wt.%)	Hydrogen recovery rate α (H_2) (%)	H_2/CO
Kraft lignin + sorbent, microwave							
1	0	CO_2	22.1	23.5	54.4	75.5	0.6
2	0	Ar	41.7	13.3	45.0	77.1	1.4
Kraft lignin + catalyst + sorbent, microwave							
3	1.45 Ni	CO_2	8.3	48.5	43.1	85.6	1.0
4	1.45 Ni	Ar	37.4	14.3	48.3	82.3	0.8
Kraft lignin + catalyst, microwave							
5	0.1 Fe	Ar	3.2	56.8	40.0	88.6	0.9
6	0.1 Fe	CO_2	3.5	54.2	42.3	87.7	0.8
7	0.1 Fe + 1.5 Ni	CO_2	3.3	56.4	40.3	90.0	0.8
Convective heating							
8	0	CO_2	38.9	19.3	41.8	83.5	0.2
9	1.5 Ni	CO_2	39.9	16.3	43.9	86.6	0.5

of the process, the kraft lignin is transformed at an average reactor temperature of 700–750°C, which is similar to the organization of the process in convective heating mode.

The application of nickel acetate to the kraft lignin did not lead to an increase in its absorptive capacity of microwave radiation; therefore, to carry out the experiments, a carbon sorbent was added to the kraft lignin (exp. 3-4). The deposition of nickel increases the degree of hydrogen extraction to 82–86%, while there is a sharp change in the selectivity of the process when using carbon dioxide or argon as the gas medium. In argon, the yields of liquid and gaseous products are identical to those obtained by the destruction of unmodified kraft lignin in argon. When carbon dioxide is used as an eluent gas, there is a sharp decrease in the yield of liquid products to 8.3% and an increase in the selectivity of the formation of synthesis gas to 73%, with a molar ratio of hydrogen to carbon monoxide equal to 1. The observed increase in the yield of hydrogen-containing gas is probably due to the catalytic action of nickel, which intensifies the process of interaction of kraft lignin and liquid products of its destruction (guaiacyl, phenyl, and vanillin derivatives) with carbon dioxide, which leads to an increase in synthesis gas output [14–17].

The application of a small amount of iron (0.1°wt.%) to kraft lignin led to a sharp increase in the absorptive capacity of microwave radiation, which was expressed in the dynamics of heating (Figure 1) and the conversion of kraft lignin in the absence of carbon material. Modification of kraft lignin with iron at MWI leads to a decrease in the yield of the fraction of liquid hydrocarbons to 3% and an increase in the yield of gaseous products (Tables 1 and 2). The yields

Table 2: The composition of the gaseous products of the conversion of kraft lignin.

No.	Active component (wt.%)	Atmosphere	Composition of the gaseous products (mol %)			
			H_2	CO	CH_4	C_2–C_4
		Kraft lignin + sorbent, microwave				
1	0	CO_2	26.2	46.3	23.9	3.5
2	0	Ar	50.8	27.8	19.6	1.8
		Kraft lignin + catalyst + sorbent, microwave				
3	1.45	CO_2	43.4	45.0	10.3	1.4
4	1.45	Ar	42.9	32.9	21.4	2.7
		Kraft lignin + catalyst, microwave				
5	0.1 Fe	Ar	35.4	39.5	19.0	6.0
6	0.1 Fe	CO_2	35.4	45.6	15.3	3.8
7	0.1 Fe + 1.5 Ni	CO_2	39.9	51.1	7.7	1.3
		Convective heating				
8	0	CO_2	12.3	56.4	28.4	3.0
9	1.5 Ni	CO_2	25.5	49.1	23.0	2.4

of liquid and gaseous products obtained during the destruction of iron-modified kraft lignin in argon and carbon dioxide are identical, which indicates a high intensity of the process when plasma is initiated directly in the kraft lignin body as well as it was observed earlier [18]. However, as compared with argon in carbon dioxide, an increase in the selectivity of the formation of synthesis gas from 64 to 72% and a proportional decrease in the selectivity of the formation of light hydrocarbons are observed. Those light hydrocarbons are actually carbon dioxide reformed under experimental conditions.

In order to increase the depth of processing of kraft lignin and increase the yield of hydrogen on kraft lignin, a combined method was used: 1.45% by weight of nickel was applied to kraft lignin containing 0.1% iron. Catalytic tests showed an increase in the degree of extraction of hydrogen to 90%, a yield of hydrogen to 22.5°wt.%, and the ratio H_2/CO-1. The yield of solid residue remained almost unchanged (Table 1).

When modifying kraft lignin with iron, it begins to absorb microwave radiation and the plasma originates directly in the kraft lignin body, i.e., the effect of microwave irradiation becomes maximum. It can be assumed that on the nickel- and iron-containing centers, the methoxy-end groups and the gaseous organic molecules formed from kraft lignin, which are identified by convective heating, undergo reforming. At the same time, an increase in the conversion and yield of synthesis gas in the presence of nickel-containing centers in the CO_2 medium compared with the results obtained when generating plasma on unmodified kraft lignin and also kraft lignin modified by nickel in Ar indicates the plasmacatalytic nature of carbon dioxide reforming.

Comparison of the conversion of the modified and the initial kraft lignin in the conditions of MV stimulation and convective heating shows that the yield of the solid residue in both cases is almost unchanged, i.e., the depth of processing of kraft lignin does not depend on the mechanism of energy transfer. However, there is a significant change in the selectivity of the formation of liquid and gaseous products. During convective heating, the yield of liquid organic products increases to 40%, which, as in the case of microwave exposure, is represented by phenyl, guaiacyl, and vanillin derivatives [19]. The hydrogen yield for the modified Ni and initial kraft lignin is 4.2 and 2.4°wt.%, respectively. When convectively heated, the CO yield for the initial kraft lignin and kraft lignin modified with nickel is 8–11°wt.%, which corresponds to the yield of carbon monoxide in the microwave conversion of unmodified kraft lignin. It is worth noting that deposition of nickel or iron on the kraft lignin under microwave irradiation conditions leads to a sharp increase in the CO yield up to 20–30°wt.%, most likely as a result of the intensification of the interaction of carbon dioxide with kraft lignin dehydrogenation products. The obtained result indicates the plasmacatalytic nature of the course of carbon dioxide reforming of kraft lignin during microwave irradiation. Quantitative analysis of liquid products is difficult because nonvolatile products are present in the mixture, which are not desorbed from the chromatographic column. In addition, repolymerization processes in liquid products also lead to the formation of nonvolatile compounds. The obtained GCMS spectra for all liquid products are identical, a typical spectrum is presented in Figure S1, and its identification is presented in Table S1.

Thus, the experimental data obtained show that the role of the carbon material (SGC) is to convert the energy of electromagnetic waves into thermal energy (Tables 1 and 2, exp. No. 1-2, 8). The plasma ignites inside the sorbent; therefore, hot spots (local overheating) occur inside the sorbent. From the hot spots, heat is transferred to the entire volume of the reactor, i.e., kraft lignin is actually converted at an average reactor temperature of 700°C. At this temperature, the endothermal Boudoir reaction (Scheme 1) proceeds slowly (exp. 2). When external CO_2 is introduced into the system (exp. 1), the equilibrium is likely to shift towards the formation of CO. The output of CO increases from 3 to 11% at T = const. in argon and carbon dioxide, respectively.

The composition and quantity of the products obtained during the conversion of unmodified kraft lignin in a mixture with SGC are identical to those obtained during convective heating (exp. 8). Therefore, the likely nature and driving force of chemical processes is the same.

$$C + CO_2 \rightleftharpoons 2CO \quad \Delta H^0_{298} = +172{,}4\ \text{kJ/mol}$$

Scheme 1: The reaction of Boudoir.

When applied to nickel kraft lignin (Exp. 3, 4, 9), during its conversion, a carbon residue enriched in metal is formed. Nickel on the residual carbon lowers the activation energy of the Boudoir reaction, which does not affect the equilibrium position, but leads to its earliest achievement. Therefore, with the introduction of nickel into the composition of kraft lignin in argon, there is a slight increase in the yield of CO, and in the medium of CO_2, the yield increases severalfold. The difference in the output of CO for exp. 3 and 9 is probably due to the fact that, in the conditions of microwave radiation and convective heating in the reactor, there is a different temperature gradient. Thus, when a catalyst is introduced, temperature fluctuations in a small range have a much greater effect on the yield of products than in a noncatalytic experiment.

The deposition of iron initiates plasma nucleation in the volume of kraft lignin (exp. 5, 6, and 7). Thus, inside the substrate, the temperature significantly exceeds the temperature determined in the reactor. An increase in temperature leads to a shift in the equilibrium of the Boudoir reaction towards the formation of CO. Comparison of experiments 5 and 6 shows that the output of CO in them is approximately equal, since it is formed of carbon monoxide, mainly due to internal oxygen and only slightly (~2%) due to external carbon dioxide. When nickel is introduced (exp. 7), the yield of CO increases by another 4%, probably due to the catalytic action of nickel. It can even be assumed that, under the reaction conditions, a CO yield of 29% (exp. 7) is close to equilibrium.

X-Ray diffraction data showed that the phase compositions of initial kraft lignin and iron-modified kraft lignin before and after catalysis are quite similar. Along with the substantial amount of organic phase, the samples contain SiO_2 and aluminum silicate phase $K_{0.93}Fe_{0.27}Al_{0.75}Si_{3.01}O_8$. After reforming, the reflections assigned to ferric carbide compounds and carbon appear. The detailed examination made it possible in identifying certain crystallographic planes for γ-Fe stabilized by carbon, $C_{0.12}Fe_{1.88}$ and $C_{0.09}Fe_{1.91}$. The reflections which can be referred to Fe_3O_4, hexagonal graphite, and orthorhombic carbon have been also observed.

Transmission electron microscopy (TEM) and Mössbauer spectroscopy examination as well as magnetic measurements have been carried out before and after reforming for samples 3, 6, and 7 (Tables 1 and 2) with supported iron concentrations of 0.5, 2.0, and 2.8°wt. %, respectively.

According to the TEM data, samples 3 and 6 obtained by impregnation of kraft lignin with $Fe(OAc)_3$ solution contain Fe-nanoparticles. The size of these particles varies in the range from 1 up to 4 nm; besides, more than 80% of them are as large as 1 ± 0.3 nm. Unlike single particles observed on the surface of samples 3 and 6, most particles of sample 7 obtained by impregnation with Fe-containing organosol, appeared to be in close contact with one another and formed extended chains and agglomerates. The average size of detectable particles in this sample is 3 nm. During the reaction, the microstructure of samples 3, 6, and 7 undergoes considerable changes. MWI-assisted heating of the reaction mixture causes particle agglomeration approximately from 1 up to 6 nm. Interestingly, about 45% Fe-containing nanoparticles in sample 3 (0.5 wt.% Fe) and 30% in sample 6 (2.0% wt.% Fe) are of core-shell structure. The Fe/C intensity ratio for the EDA spectra of particle edge and center shows that the core mainly consists of iron, whereas the shell is highly enriched in carbon. HRTEM image of the core-shell particle on the kraft lignin surface after reforming of sample 6 is presented in Figure 4. The formation of core (Fe)-shell(C) particles is apparently due to kraft lignin destruction under MWR and plasma conditions on Fe particles followed by enveloping the particle surface by carbon-containing fragments. The calculation of interplanar spacing d for the shell of such a particle yields $d = 3.6$ Å, which coincides with d for the C(002) face. The faces with $d = 1.47$, 2.43, 3.6, and 4.2 Å are also present on the particle surface. Considering the measurement error (±0.3 Å) and the possibility of dissolution of some carbon in Fe-containing oxide, the interplanar spacings of 4.2, 2.43, and 1.47 Å can be assigned to Fe_3O_4 identified by X-ray diffraction as well.

The Mössbauer spectroscopy and magnetic measurements shed light on the complex electronic structure and cooperative spin interactions in the system of Fe-containing nanoparticles before and after experiment. These results also can help to reveal the main difference between the Fe-containing nanoparticles structure formed on the surface of kraft lignin with and without nickel addition.

The most significant distinctive feature of the Mössbauer spectrum recorded after microwave radiation is the presence of a single line with the isomer shift $\delta = -0.08$ mm/s characteristic of small γ-Fe clusters or, more precisely, γ-Fe-Cn clusters [20, 21]. Under MWI, a considerable fraction of small, ~1–3 nm, superparamagnetic clusters are agglomerated forming larger superparamagnetic clusters of nonstoichiometric magnetite with a relative content of ~30–35%. Another distinctive feature of the spectrum for the sample obtained using impregnation from $Fe(OAc)_3$ solution recorded after reforming is the presence of a single line with the isomer shift $\delta = -0.08$ mm/s, which is characteristic for small γ-Fe clusters or, more precisely, γ-Fe-C_n clusters (Table 3) [22, 23]. The area of the γ-Fe-C_n single line is ~20% of the area of the whole spectrum. Since sample 6 contains ~30% of core-shell particles according to TEM examination, it can be roughly estimated that the iron-carbon compounds are formed exactly in these particles. The reflections for the iron-carbon compounds and Fe_3O_4 are also detected in the X-ray diffraction patterns.

The magnetic measurements in $H = 39.8$ kA/m did not reveal any difference in magnetic behavior of the samples obtained by impregnation from $Fe(OAc)_3$ and $Fe(OAc)_3 + Ni(OAc)_2$ solution (Figure 5(a)). The careful magnetic characterization of these samples showed that they

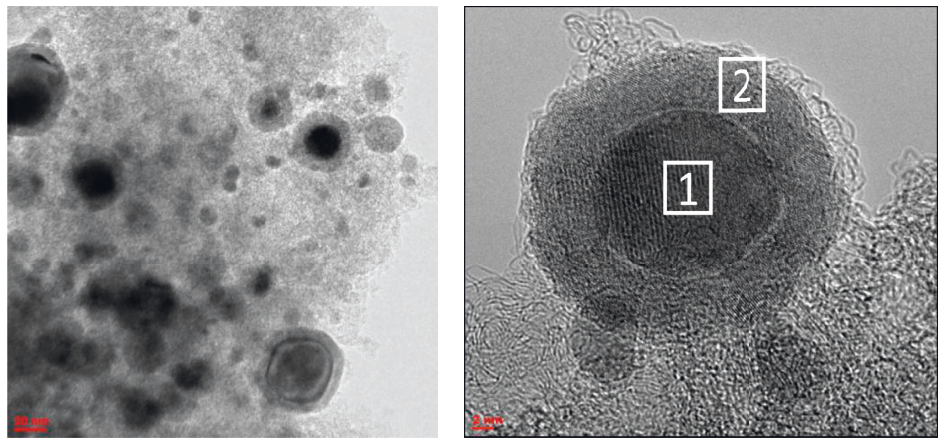

(a) (b)

Figure 4: (a, b) Micrographs of active components after the reaction.

Table 3: Mössbauer parameters of the spectra at T = 300 K of samples 0.1 Fe/(kraft lignin) and 0.1 Fe–1.5 Ni/(kraft lignin) before and after the experiments.

Sample	Fe form	δ ±0.03 mm/s	Δ ±0.03 mm/s	H_{in}, T ±0.5T	A (%) ±0.05
0.1 Fe/(kraft lignin)-initial	Fe^{3+} (paramagn.)	0.36	0.73	—	0.82
	Fe^{2+} (paramagn.)	0.74	1.10		0.18
0.1 Fe/(kraft lignin)-solid rest after experiment	Fe^{3+} (paramagn.)	0.38	1.00	—	0.52
	$Fe_3O_{4+\delta}$ (A)*	0.35	0.03	48.7	0.13
	$Fe_3O_{4+\delta}$ (B)*	0.66	0.02	44.8	0.17
	FeO (paramagn.)**	−0.08	—	—	0.18
0.1 Fe-1.5 Ni/(kraft lignin)-initial	Fe^{3+} (paramagn.)	0.36	0.89	—	1.00
0.1 Fe-1.5 Ni/(kraft lignin)-solid rest after experiment	Fe^{3+} (paramagn.)	0.36	0.87	—	0.62
	Fe^{2+} (paramagn.)	0.66	1.61	—	0.10
	$Fe_3O_{4+\delta}$ (A)*	0.26	-0.02	48.4	0.12
	$Fe_3O_{4+\delta}$ (B)*	0.69	0.04	45.7	0.16

*A (tetrahedral) and B (octahedral) sites of superparamagnetic clusters of nonstoichiometric magnetite; **possibly γ-Fe-C. δ is an isomeric shift relative to a-Fe; Δ is the quadrupole splitting or quadrupole shift; H_{in} is the internal magnetic field on 57 Fe nucleus; A is the relative content.

are overall paramagnetic. Meanwhile, the measurements in low magnetic field, H = 39.8 kA/m, showed that unlike Fe/(kraft lignin) sample, the FC and ZFC curves for Fe-Ni sample diverge at T = 97 K and at T = 8 K, a magnetic phase transition occurs (Figure 5(a)). We argue that magnetic properties of Fe-Ni/(kraft lignin) samples are characteristic for the superparamagnetic system of Fe-containing particles. It should be mentioned that Ni-containing nanoparticles deposed on kraft lignin surface and Fe-containing particles demonstrate similar magnetic behavior. The magnetic characterization including the dependence of magnetization, M, on the magnetic field for the Fe–Ni/(kraft lignin) and Fe/(kraft lignin) (Figure 5(b)) confirms X-ray, TEM, and Mössbauer spectra data, pointing to that the phase composition of deposited active components consists of about 60% of Fe_3O_4 nanoparticles and also of ~40% of the core (Fe_3O_4)@shell (nonstochiometric γ-Fe-C_n) nanostructures.

4. Conclusion

As was shown in [13, 14], the microwave effect, which leads to plasma generation, is dominated by the C–H bond between organic substrates, which is fully confirmed in the case of kraft lignin. Thus, the main difference between the modes of convective heating and microwave exposure is to change the selectivity of the process, which can be directed towards the formation of liquid organic substrates during convective heating and towards the formation of hydrogen-containing gas in the case of microwave exposure.

When iron is applied to kraft lignin, the chemistry of kraft lignin destruction changes—the degree of hydrogen extraction increases and the formation of CO occurs due to the internal (own) oxygen of kraft lignin, and not CO_2. The reason is the generation of plasma and the formation of hot

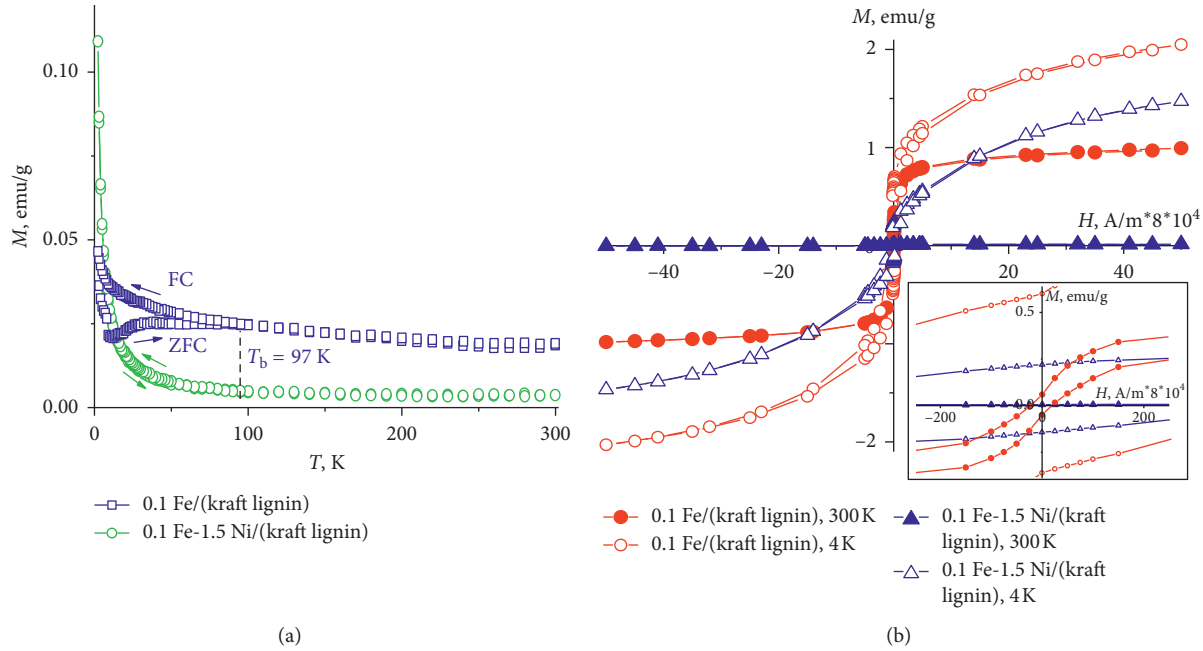

FIGURE 5: (a) Temperature dependence of the magnetization (M) in a H = 39.8 kA/m field for initial (before the reforming) of samples 0.1 Fe/(kraft lignin) (○) and 0.1 Fe-1.5 Ni/(kraft lignin) (□) recorded in the FC and ZFC modes. The inset shows the M(T) curves for samples 3, 6, and 7 measured in a H = 39.8 kA/m field; (b) M(H) curves for samples 3 and 6 at T = 300 and 4 K after the reforming. The inset shows the hysteresis loops for low fields at T = 300 and 4 K (residual M_r = 0.6 emu/g and M_r = 0.06 emu/g for 4 and 300 K, respectively; saturation M_s = 1.51 emu/g and M_s = 0.84 emu/g for 4 and 300 K, respectively).

spots occur in the kraft lignin body; therefore, the true temperature of its destruction is higher than when using a sorbent, where the plasma originates in the body of the sorbent.

Data Availability

The data used to support the findings of this study are available from the corresponding author upon request.

Conflicts of Interest

The authors declare that they have no conflicts of interest.

Acknowledgments

This work was done with the financial support of the Ministry of Science and Higher Education of the Russian Federation for the project part of the State Task (Subsidy Agreement no. 14.613.21.0073 of October 23, 2017, unique number: RFMEFI61317X0073).

Supplementary Materials

Quantitative analysis of liquid products is difficult because nonvolatile products are present in the mixture, which are not desorbed from the chromatographic column. In addition, repolymerization processes in liquid products also lead to the formation of nonvolatile compounds. The obtained GCMS spectra for all liquid products are identical, a typical spectrum is presented in Figure S1, and its identification is presented in Table S1. (*Supplementary Materials*)

References

[1] R. M. Rowell, R. Pettersen, J. S. Han, J. S. Rowell, and M. A. Tshabalala, "Cell wall chemistry," in *Handbook of Wood Chemistry and Wood Composites*, R. M. Rowell, Ed., pp. 9–40, Taylor and Francis Group, Boca Raton, FL, USA, 2005.

[2] W.-J. Liu, H. Jiang, and H.-Q. Yu, "Thermochemical conversion of lignin to functional materials: a review and future directions," *Green Chemistry*, vol. 17, no. 11, pp. 4888–4907, 2015.

[3] M. L. Rabinovich, "Wood hydrolysis industry in the Soviet union and Russia: what can Be learned from the history?," in *Proceedings of 2nd Nordic Wood Biorefinery Conference*, pp. 111–120, Helsinki, Finland, September 2009.

[4] T. Q. Hu, *Chemical Modification, Properties, and Usage of Kraft Lignin*, Springer, Berlin, Germany, 2002.

[5] M. V. Tsodikov, M. A. Perederiy, M. S. Karaceva et al., "Formation of iron-containing catalysts on carbon carriers under the influence of microwave radiation," *Nanotechnologies in Russia*, vol. 1, p. 161, 2007.

[6] A. J. Buttress, E. Binner, C. Yi, P. Palade, J. P. Robinson, and S. W. Kingman, "Development and evaluation of a continuous microwave processing system for hydrocarbon removal from solids," *Chemical Engineering Journal*, vol. 283, pp. 215–222, 2016.

[7] J. Robinson, C. Dodds, A. Stavrinides et al., "Microwave pyrolysis of biomass: control of process parameters for high pyrolysis oil yields and enhanced oil quality," *Energy and Fuels*, vol. 29, no. 3, pp. 1701–1709, 2015.

[8] Q. Bu, H. Lei, L. Wang et al., "Bio-based phenols and fuel production from catalytic microwave pyrolysis of lignin by activated carbons," *Bioresource Technology*, vol. 162, pp. 142–147, 2014.

[9] L. Fan, P. Chen, Y. Zhang et al., "Fast microwave-assisted catalytic co-pyrolysis of lignin and low-density polyethylene with HZSM-5 and MgO for improved bio-oil yield and quality," *Bioresource Technology*, vol. 225, pp. 199–205, 2017.

[10] S. Liu, Q. Xie, B. Zhang et al., "Fast microwave-assisted catalytic co-pyrolysis of corn stover and scum for bio-oil production with CaO and HZSM-5 as the catalyst," *Bioresource Technology*, vol. 204, pp. 164–170, 2016.

[11] W. Yunpu, D. Leilei, F. Liangliang, S. Shaoqi, L. Yuhuan, and R. Roger, "Review of microwave-assisted lignin conversion for renewable fuels and chemicals," *Journal of Analytical and Applied Pyrolysis*, vol. 119, pp. 104–113, 2016.

[12] F. Mushtaq, R. Mat, and F. N. Ani, "A review on microwave assisted pyrolysis of coal and biomass for fuel production," *Renewable and Sustainable Energy Reviews*, vol. 39, pp. 555–574, 2014.

[13] M. V. Tsodikov, M. A. Perederii, A. V. Chistyakov, G. I. Konstantinov, and B. I. Martynov, "Degradation of organophosphorus compounds adsorbed in carbon sorbent pores," *Solid Fuel Chemistry*, vol. 46, no. 1, pp. 37–44, 2012.

[14] K. H. Kim, A. Farooq, M. Y. Song et al., "Acetaldehyde removal and increased H2/CO gas yield from biomass gasification over metal-loaded Kraft lignin char catalyst," *Journal of Environmental Management*, vol. 232, pp. 330–335, 2019.

[15] Y. Xie, Y. Su, P. Wang, S. Zhang, and Y. Xiong, "In-situ catalytic conversion of tar from biomass gasification over carbon nanofibers- supported Fe-Ni bimetallic catalysts," *Fuel Processing Technology*, vol. 182, pp. 77–87, 2018.

[16] L. F. Xie, P. G. Duan, J. L. Jiao, and Y. P. Xu, "Hydrothermal gasification of microalgae over nickel catalysts for production of hydrogen-rich fuel gas: effect of zeolite supports," *International Journal of Hydrogen Energy*, 2018.

[17] Q. Guan, T. Mao, Q. Zhang et al., "Catalytic gasification of lignin with Ni/Al2O3-SiO2 in sub/supercritical water," *Journal of Supercritical Fluids*, vol. 95, pp. 413–421, 2014.

[18] M. V. Tsodikov, G. I. Konstantinov, A. V. Chistyakov, O. V. Arapova, and M. A. Perederii, "Utilization of petroleum residues under microwave irradiation," *Chemical Engineering Journal*, vol. 292, pp. 315–320, 2016.

[19] F.-X. Collard and J. Blin, "A review on pyrolysis of biomass constituents: mechanisms and composition of the products obtained from the conversion of cellulose, hemicelluloses and lignin," *Renewable and Sustainable Energy Reviews*, vol. 38, pp. 594–608, 2014.

[20] O. V. Arapova, G. N. Bondarenko, A. V. Chistyakov, and M. V. Tsodikov, "A study of the structural changes in kraft lignin by vibrational spectroscopy under the influence of microwave radiation," *Journal of Physical Chemistry*, vol. 9, pp. 1520–1533, 2017.

[21] B. David, N. Pizúrová, O. Schneeweiss, V. Kudrle, O. Jašek, and P. Synek, "Iron-based nanopowders containing α-Fe, Fe3C, and γ-Fe particles synthesised in microwave torch plasma and investigated with mössbauer spectroscopy, Japan," *Japanese Journal of Applied Physics*, vol. 50, no. 8, article 08JF11, 2011.

[22] Y. Yao, L. K. L. Falk, R. E. Morjan, O. A. Nerushev, and E. E. B. Campbell, "Synthesis of carbon nanotube films by thermal CVD in the presence of supported catalyst particles. Part II: the nanotube film," *Journal of Materials Science: Materials in Electronics*, vol. 15, no. 9, pp. 583–594, 2004.

[23] Y. Yamada, H. Yoshida, K. Kouno, and Y. Kobayashi, "Iron carbide films produced by laser deposition," *Journal of Physics: Conference Series*, vol. 217, p. 01209, 2010.

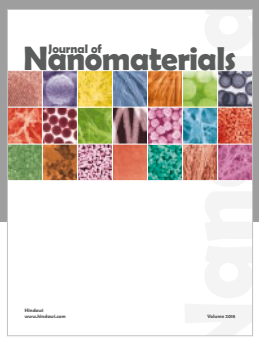

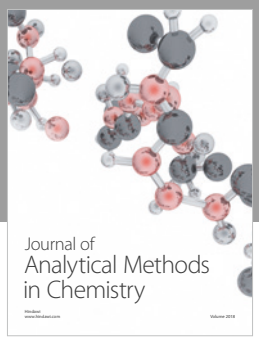

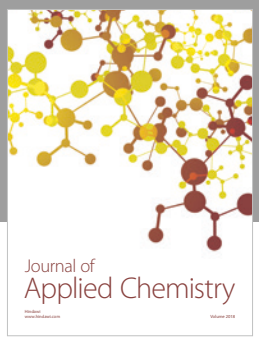

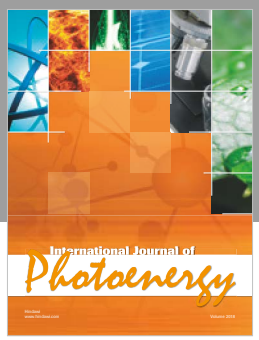

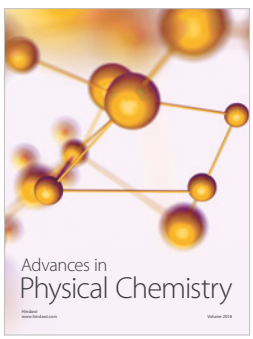

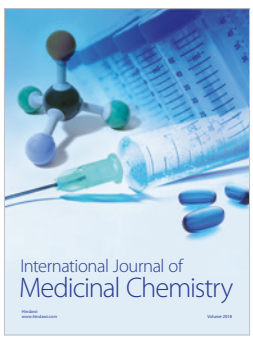

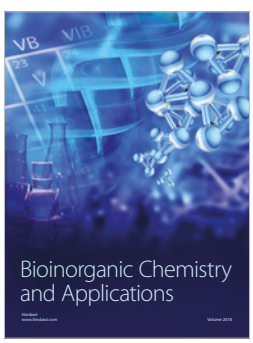

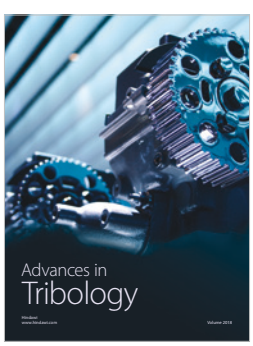

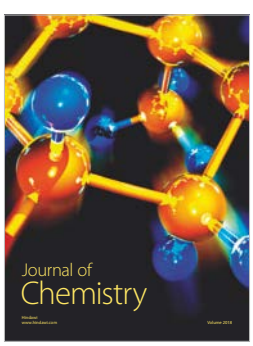

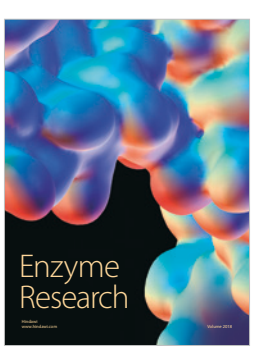

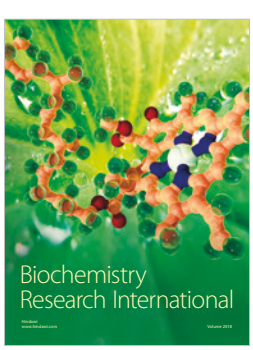

Hindawi

Submit your manuscripts at
www.hindawi.com